Jurnal Geofisika (2025) Vol. 23, No. 1 hal. 23-32

Performance Evaluation of ADS 1256 for Geoelectric Data Acquisition System: Laboratory Scale Comparative Study

Yudha Agung Pratama[1] dan Suharsono[1]
[1]Department of Geophysical Engineering, Faculty of Mineral and Energy Technology, Universitas Pembangunan Nasional "Veteran" Yogyakarta

*Email: yudha.agung@upnyk.ac.id; harsonomgl@upnyk.ac.id

Submit: 6 Juli 2025; Revised: 6 September 2025; Accepted: 9 September 2025

Abstract: *The need of flexible and affordable geoelectric data acquisition systems is growing, particularly for research and educational purposes. This study aimed to evaluate the performance of a resistance measurement system based on the ADS1256 high-precision ADC module on a laboratory scale. Initial testing was conducted on a laboratory scale using various resistance values. The best accuracy was found in the medium to high resistance range R1 (subsurface target) (> 10Ω); at low resistance, the accuracy value decreased dramatically. A relative error (ε) reading of - 6.7% occured at low values of R1. The condition of the resistance R2 (surface) affected the stability of the ADS 1256 system reading. Based on the standard deviation value $S_{\overline{x}}$ there was an indication of nonlinearity in the readings, particularly in the voltage readings. The current measurements produced relatively stable readings. There was an increase in the fluctuation of $S_{\overline{x}}$ readings, especially at low surface medium (R2). Overall, the ADS1256 system demonstrated promising potential as a low-cost alternative for resistance measurement, particularly effective in the medium to high resistance range. Comprehensive data across all R1 and R2 variations require additional calibration and enhanced circuit stability to better align with reference values*

Keywords: *ADS1256, accuracy, geoelectric.*

1 INTRODUCTION

One of the main reasons for developing geoelectric equipment is the high price of commercial devices currently available. These devices are often designed as closed systems, which limits the possibility of modification to suit research needs. This condition can become an obstacle, especially for researchers and institutions with restricted budgets (Clement et al., 2020).The development of user-friendly measurement tools, assembled from easily accessible electronic components, could simplify data acquisition in frequency-dependent soil property studies, rivaling the ease of regular low-frequency resistivity measurements (Kuklin, 2020). Research on the development of local-scale geoelectric instrument designs has been conducted to overcome challenges such as the need for multidisciplinary research in addressing complex problems in social and physical sciences (Muhammad and Gunawan, 2016; Azharudin et al., 2013; Hazreek et al., 2017). The study focused on the construction of the basic system and its application. Further testing of the electrical system of geoelectric devices, especially on the aspect of the current used is essential to characterize the system's behavior in both homogeneous and heterogeneous soil samples (Indarto et al., 2016; Fatima-Zohra et al., 2019). In shallow subsurface exploration, resistivity patterns—largely governed by the nature of fluids and the interconnectedness of pores—provide critical insights into underlying structures, reinforcing the role of resistivity techniques (Saad et al., 2010). Electrical resistivity tomography and electromagnetic induction techniques are particularly useful for imaging flow patterns in the unsaturated zone, due to the sensitivity of electrical resistivity to subsurface soil moisture (De-Carlo et al., 2021). In parallel, components of the data storage system were examined to enhance the efficiency of data handling, transfer, and archival, thereby maintaining the integrity and availability of geoelectric data for future research use (Clement et al., 2020; Hartono et al., 2022).

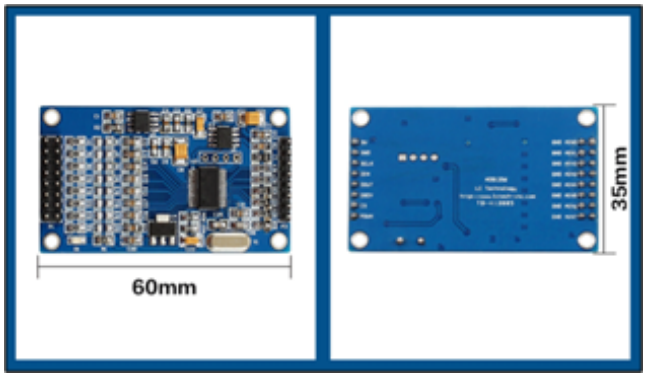

Figure 1. ADS1256 24-bit 8-channel high precision Modul ADC (ChinalcTech, 2023)

Current geoelectric tool development efforts are not only limited to functional testing of supporting devices, but also directed at improving the accuracy of the measurement system across a spectrum of resistance values, with a specific focus on reducing the influence of electrode–soil contact resistance (Zhao and Anderson, 2018). One approach is to utilize high-precision voltage sensors and ADC (Analog-to-Digital Converter) modules. Nasution and Lubis (2023) reported that the use of INA219 voltage sensors resulted in a

Table 1. Parameters of the resistivity geoelectrical method (adapted from Telford et al. (1990))

Geologic Material	Resistivity (ohm.m)
Soil	2 – 300
Clay (wet)	1 – 50
Clay (dry)	10 – 100
Sand (wet)	1000 – 10000
Sand (dry)	50 – 500
Sandstone	50 – 1000
Shale/Siltstone	10 – 400
Limestone/Dolomite	1000 – 10000
Granite	1000 – 10000
Metamorphic rocks	300 – 3000
Air	Very large
Water (fresh)	50 – 100
Water (salty)	0.2

Table 2. Variations in R1 and R2 values used

R2 (Ω)	R1 (Ω)
50	1
100	5
470	20
1000	100
2000	470
3000	2000

potential measurement accuracy of 96% and a current accuracy of 83%. Meanwhile, Setiawan et al. (2024) reported an accuracy of 97.44% for voltage and 97.28% for current. On the other hand, the use of the ACS712 current sensor still shows limitations, with an average error of 9.53% (Huda et al., 2021). The use of 16-bit ADCs, such as the ADS1115, does not provide optimal results, with Rahman et al. (2025) reporting an average error of 54%.

The majority of locally created prototypes are still limited to 16-bit ADCs, which makes it difficult for them to precisely resolve tiny geoelectric signals. The use of a 24-bit ADC in comparable local instrumentation has not yet been documented. Moreover, to the best of our knowledge, there has been no systematic evaluation of the ADS1256 performance in geoelectric measurements, particularly in the R1–R2 configuration. By using the ADS1256, a 24-bit high-resolution ADC intended for precise measurements, this study addresses that gap. Compared with 16-bit devices, the ADS1256 provides markedly higher resolution, offers eight analog input channels, supports differential measurements, and uses a programmable gain amplifier (PGA) to strengthen weak signals before conversion. Its ability to record tiny currents and delicate geoelectric potentials is further enhanced by its 30,000 samples per second (SPS) sampling capacity. The novelty of this work lies in the application of a higher-resolution ADC to locally developed geoelectric instruments, thereby overcoming the accuracy issues found in earlier 16-bit prototypes.

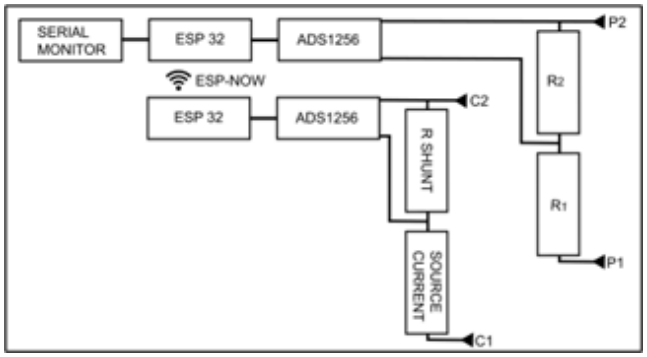

Figure 2. Circuit separation for potential and current measurements, controlled via an ESP32 Wi-Fi module.

2 METHOD

2.1 Testing Design

To determine the quality of data generated by the ADS1256 module-based geoelectric measurement system Figure 1, the assessment focused on the precision and accuracy parameters of the measurement results. The specific resistance value was used as the dependent variable, with a 20W 5% ceramic resistor as the test material. To improve accuracy, measurements were made using a reference standard. The variation in the resulting reading value acts as the independent variable and is analyzed descriptively through the calculation of the mean value and standard deviation of the measurement. Accuracy is assessed by comparing the average reading with the reference resistance to obtain absolute and relative errors, while precision and consistency are evaluated through the measurement's standard deviation. Since the use of dummy resistors can increase the temperature of the test resistors, temperature measurements are performed using a K-type thermometer to maintain temperature stability and ensure data quality. Materials and devices used in this study:

(a) Fluke 116 multimeter as a reference
(b) DC - DC step up as a current source
(c) Laptop (PC) for program and data viewer
(d) ESP32 microcontroller (MCU)
(e) ADC ADS1256
(f) Relay Module
(g) Resistor, consisting of R 20W 5%, R voltage divider, and R shunt
(h) Thermometer Type K TM-902C
(i) Cables and connectors

The microcontroller is programmed to run the ADC acquisition process. The measurement design employed involves designing an acquisition system to measure two parameters simultaneously: potential difference and current strength. In this study, researchers used an ESP32 MCU to program the acquisition system. Programming was carried out using the Arduino IDE software, which regulates each ADC function, including the recording type (differential or single-ended), channel selection, recording start time, sampling rate, gain adjustment via PGA (Programmable Gain Amplifier), and communication between microcontrollers. The data acquisition process also involves controlling several relays to activate the current injection and define the measurement

Table 3. Measurement of resistance as a benchmark using a Fluke 116 with an accuracy of 0.9% + 1 digit

R 5%	R Value by Fluke U in Ω	0.9% uncertainty U in Ω	1 digit U in Ω	Total uncertainty U in Ω	$U + u$	Relatif uncertainity δ_r in %	Suitability
1	1.1	0.0099	0.1	0.10	1.1 ± 0.1	10.9	Not suitable
5	5.2	0.0468	0.1	0.15	5.2 ± 0.15	2.93	Borderline
20	20.1	0.1809	0.1	0.28	20.1 ± 0.28	1.40	Acceptable
100	101.6	0.9144	0.1	1.01	101.6 ± 1.01	1.01	Good
470	476.1	4.2849	0.1	4.38	476.1 ± 4.38	0.93	Very Good
2000	1971.9	17.7471	0.1	17.84	1971.9 ± 4.38	0.89	Excellent

timing. The measurement data is subsequently stored and read through the serial monitor.

The variation of the R1 range was utilized to perform the testing, with R1 and R2 selected to correspond to the resistivity measurement range under actual conditions as presented in Table 1. In practical measurements, two resistance values may be obtained. Resistance R1 represents the subsurface medium that serves as the target (datum point), whereas Resistance R2 represents the surface medium, corresponding to the electrode contact resistance.

The selection of R1 and R2 values was based on the resistivity range presented in Table 2. The resistance values employed in the testing were adjusted to match the common ranges typically encountered in resistivity measurements. In this experiment, the geometry factor was set to k = 1, allowing the measured values to be assumed as resistivity values. The determination of resistivity also considered the availability of ceramic resistor components in the market, as presented in Table 2. These resistors are assumed to adequately represent the range of low- and high-resistivity media variations for each R1 and R2 value.

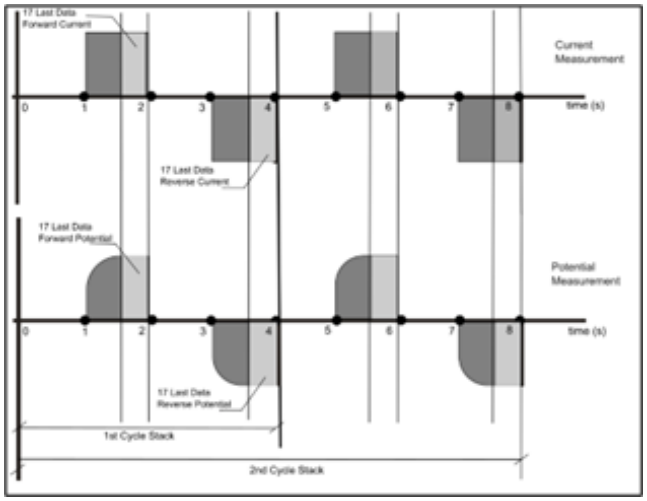

Figure 3. Measurement cycle in a two-channel geoelectric data acquisition, displaying current (top) and potential (bottom) readings over time. Two stacks were recorded, yielding 68 data points.

2.2 Analysis Method

This analysis aims to develop a systematic approach for assessing the readout quality of the designed system utilizing the ADS1256. The analysis process involves calculating the absolute error and relative error of the readout results. The absolute error is defined as $\xi = \tilde{A} - A$, with A as the reference value and $\tilde{A}$ as the measured value. The absolute error value can be positive or negative, whereas the absolute value of the error is always positive. The relative error is expressed as $\varepsilon = \left(\tilde{A} - A\right)/A$ in units of percent (%). To obtain the error value, the reference resistance (A) of the R1 value is used. The reference values of R1 were obtained through measurements using a Fluke 116 multimeter as a benchmark. This tool has an accuracy (u) specification of ±0.9% + 1 digit, and the measurement results are expressed in the form $U \pm u$. The results of measuring resistance R1 with the Fluke 116 are shown in Table 2.

The relative uncertainty value $\delta_r = u/U$ is shown as a percentage. The Fluke 116 has limitations in low resistance measurements (e.g., 1 Ω), where the relative uncertainty value can reach 10.9%, thus widening the reference error range. The table also presents the maximum acceptable error limits for each resistance value. In general, the relative uncertainty value gets smaller at higher resistances, indicating the quality limit of the reference benchmark at each resistance value R1.

$$S(\tilde{x}) = \sqrt{\frac{\sum_{i=1}^{n}(x_i - \tilde{x})^2}{n-1}} \quad (1)$$

The number of replicates of the data was done to ensure reliability and allow statistical analysis of the mean $e\tilde{x}$ and standard deviation $S(\tilde{x})$.

The the potential (mV) and current (mA) data were collected in 8 replicates per test configuration. The absolute value of error ξ for resistance R1 using the ADS1256 system is calculated by comparing the calculation results based on Ohm's law $R = V/I$, which is the ratio between the voltage and current readings. The standard deviation value $S(\tilde{x})$ of the reading results is also calculated and compared for each configuration variation R1 and R2. The system determines the absolute error ξ and relative error (ε) % values for R1 by comparing the ADS1256 system measurement results to the reference values obtained from the Fluke multimeter readings.

3 RESULT

Measurements using the ADS1256 system were made at various variations of R1 and R2 values. Table 4 shows one of the variations in potential and current measurement results. The value of R1 was fixed at 1.1 Ω, while R2 was varied

Table 4. Results table n- data on ground resistance 1.1 Ω

(a) Potential (mV)

R1 reference U in Ω		R2 (Ω)					
		50	100	470	1000	2000	3000
1.1	n1	931	549	137.9	23.68	12.24	8.19
	n2	941	547	138.0	23.68	12.22	8.18
	n3	936	548	138.1	23.68	12.22	8.05
	n4	932	546	138.1	23.69	12.23	7.86
	n5	926	544	137.9	23.70	12.22	7.92
	n6	933	547	138.0	23.69	12.22	7.83
	n7	927	544	138.0	23.69	12.22	8.21
	n8	926	541	136.9	23.73	12.22	7.82
	$\bar{x}$	931.50	545.75	137.85	23.69	12.22	8.01
	$S_{\bar{x}}$	5.264	2.605	0.389	0.017	0.007	0.17

(b) Current (mA)

R1 reference U in Ω		R2 (Ω)					
		50	100	470	1000	2000	3000
1.1	n1	874	505	127.8	22.49	11.68	7.81
	n2	886	506	128.0	22.53	11.61	7.81
	n3	882	510	127.8	22.55	11.67	7.81
	n4	876	505	127.8	22.50	11.65	7.73
	n5	871	507	127.7	223.56	11.61	7.79
	n6	871	510	127.8	22.55	11.68	7.80
	n7	871	505	128.0	22.55	11.68	7.83
	n8	873	508	126.7	22.55	11.67	7.82
	$\bar{x}$	875.50	507	127.70	22.54	11.66	7.80
	$S_{\bar{x}}$	5.632	2.138	0.417	0.026	0.030	0.031

Table 5. Average values of potential and current measurements for ground resistance variations of 1.1, 5.2, 20.1, 101.6, 476.1 and 1971.9 Ω

(a) Mean Potential $\bar{x}$ (mV)

R1 reference U in Ω	R2 (Ω)					
	50	100	470	1K	2K	3K
1.1	932	546	138	24	12	8
5.2	4273	2574	248	117	61	41
20.1	15229	9444	970	465	240	159
101.6	53825	37188	4482	2254	1198	810
476.1	98138	84963	15421	9002	5116	3567
1971.9	120600	110125	31437	23147	15686	11845

(b) Mean Current $\bar{x}$(mA)

R1 reference U in Ω	R2 (Ω)					
	50	100	470	1K	2K	3K
1.1	875.5	507.0	127.7	22.5	11.7	7.8
5.2	847.0	505.9	47.3	22.5	11.6	7.8
20.1	751.8	462.5	46.6	22.3	11.6	7.8
101.6	515.3	355.9	43.0	21.5	11.4	7.7
476.1	200.7	174.2	31.9	18.3	10.4	7.2
1971.9	61.2	55.6	15.7	11.5	7.8	5.9

from 50 to 3000 Ω. The potential and current readings are presented in each row and column in the table. Values n1 to n8 represent the number of measurements. The potential reading results (mV) show an average voltage value $\tilde{x}$ that varies with the different values of resistance R2. The smaller the R2 value, the greater the potential value read. The standard deviation $S_{\tilde{x}}$ showed the highest value of 5.264 mV at low ground resistance (50 Ω), indicating a variation in reading instability. In the current reading (mA), the average current value $\tilde{x}$ increased as the value of R2 decreased. The standard deviation $S_{\tilde{x}}$ value of the current highest of 5.632 mA also occurs at R2 = 50 Ω, indicating the instability of

Table 6. Standard deviation of potential and current measurements for varying values of resistance R1 (1.1, 5.2, 20.1, 101.6, 476.1 and 1971.9 Ω)

(a) Standar Deviation Potential $S_{\bar{x}}$ (mV)

R1 reference U in Ω	R2 (Ω)					
	50	100	470	1K	2K	3K
1.1	5.3	2.6	0.4	0.0	0.0	0.2
5.2	42.0	10.1	0.1	1.9	0.0	0.3
20.1	92.8	49.0	0.3	0.1	2.0	2.9
101.6	276.5	527.6	54.7	35.1	1.9	0.2
476.1	792.7	486.8	64.4	48.0	63.3	13.5
1971.9	981.3	480.3	94.0	49.2	22.5	10.1

(b) Standar Deviation Current $S_{\bar{x}}$(mA)

R1 reference U in Ω	R2 (Ω)					
	50	100	470	1K	2K	3K
1.1	5.632	2.138	0.417	0.026	0.030	0.031
5.2	9.562	1.356	0.030	0.030	0.064	0.018
20.1	5.339	3.071	0.013	0.028	0.026	0.046
101.6	3.105	5.027	0.032	0.025	0.029	0.0277
476.1	1.451	0.980	0.016	0.031	0.011	0.033
1971.9	0.419	0.239	0.017	0.021	0.038	0.013

the current measurement in the low resistance range. An increasing trend in$S_{\bar{x}}$ readings, measured in both mV and mA, indicates decrease in the precision of the ADS1256 system when the R2 value is low. The value of R1 was changed to six different variations (1.1 to 1971.9 Ω). Table 5 presents the average values of potential and current readings obtained from each of the eight measurements. The data shows that the average $\tilde{x}$ potential (mV) and average $\tilde{x}$ Current (mA) decreases systematically as the value of R2 increases. This decrease indicates that R2 has a significant influence on the performance of the measurement system. In configurations with low R2, the average values of potential and current tend to be higher, reflecting more idealized circuit conditions. Conversely, at higher R2 values, there is a decrease in measurement performance. Based on the difference in values between the average potential and the current, it shows that the potential value has a much wider range of changes, from 8 mV to 120,600 mV. Meanwhile, the average current shows a narrower range, from 5.9 mA to 875.5 mA.

Table 6 presents the standard deviation values $S_{\tilde{x}}$ calculated from some n data. Generally, the standard deviation indicates the degree of fluctuation or instability in the readings. Based on the data, both voltage (mV) and current (mA) show greater fluctuation at low R2 values. The value of $S_{\tilde{x}}$ tends to stabilize (decrease) as the value of R2 increases. The highest standard deviation value in the potential measurement (mV), which amounted to 981.3 mV, occurred in the combination of high R1 (1971 Ω) and low R2 (50 Ω). While the highest value in current measurement (mA), which amounted to 5.632 mA, occurred in the combination of low R1 (1.1 Ω) and low R2 (50 Ω). Based on the values in the table, the pattern of standard deviation $S_{\tilde{x}}$ change can be recognized for each combination of R1 and R2. This pattern shows that measurements using the ADS1256 tend to be more volatile when R2 is low. Measurement deviations appear to be affected by variations in the values of R1 and R2.

The potential and current readings were then calculated using Ohm's Law equation to obtain the resistance value (Ω), as shown in Table 7. At R1 of 1.1 Ω, the device readings ranged from 1.03 Ω to 1.08 Ω, which is still within the reference tolerance range. Table 7 presents the absolute deviation of the measurements, which ranged from -0.073 Ω to -0.021 Ω, compared to the reference values in Table 2. In relative terms, the most significant error occurred at R2 = 3000 Ω at -6.67%, while the smallest was recorded at -1.87% at R2 = 470 Ω. Although the relative error values are still within a reasonable range for low resistances, attention is still needed, as the variation of R2 is shown to affect the stability of the readings. Ideally, the readings should remain close to 1.1 Ω regardless of the value of R2.

At R1 = 5.2 Ω, the readings showed a stable response and were quite close to the reference value, with a maximum absolute error of ±0.16 Ω. The largest relative error occurred at R2 = 50 Ω, which was -2.99%, while the smallest was recorded at +0.15% at R2 = 1000 Ω (Table 7). In general, the ADS1256 ADC performance in this range is quite good, as all relative error values are within the ±3% range; in fact, 4 out of 6 tests show an error <1%, indicating acceptable performance for medium resistance measurements. The reading values tended to be slightly lower than the reference at low R2, and increased or neutral at high R2. At R1 = 20.1 Ω, Table 6 shows that all readings were consistently above the reference value for each R2 variation. Absolute errors ranged from +0.158 Ω to +0.713 Ω, with a maximum relative error of +3.54% at R2 = 1000 Ω (Table 7).

Quantitatively, only one point (R2 = 50 Ω) has a relative error <1%, while the other points are between 1.59% and 3.54%. This trend indicates a systematic positive offset that starts to appear when the system measures resistances above 20 Ω. The possible cause is the suboptimal calibration of the linear voltage divider or potential autorange system, which causes the readings to tend to overestimate. Testing against the reference value of 101.6 Ω showed a consistent

Table 7. Absolute Error and Relative Error values of ADS1256 system resistance measurement referencing Fluke reference resistance

(a) Absolut Error ξ in Ω

R1 reference	R2					
U in Ω	50	100	470	1000	2000	3000
20	-0.036	-0.024	-0.021	-0.049	-0.051	-0.073
40	-0.156	-0.113	0.040	0.008	0.052	0.015
60	0.158	0.319	0.707	0.713	0.612	0.339
80	2.865	2.896	2.556	3.284	3.883	3.906
100	12.8	11.77	7.81	15.08	15.12	16.87
100	-1.73	7.44	30.01	34.16	36.88	32.36

(b) Relative Error ε in %

R1 reference	R2					
U in Ω	50	100	470	1000	2000	3000
20	-3.28	-2.14	-1.87	-4.42	-4.66	-6,67
40	-2.99	-2.17	0.77	0.15	1.01	0.30
60	0.79	1.59	3.52	3.54	3.05	1.69
80	2.82	2.85	2.52	3.23	3.82	3.84
100	2.69	2.47	1.64	3.17	3.18	3.54
100	-0.09	0.38	1.52	1.73	1.87	1.64

increase in absolute and relative error across the R2 variations. All tool reading values were above the reference value, with absolute errors ranging from +2.556 to +3.906 Ω, and relative errors ranging from +2.52% to +3.85%, as shown in Table 7. This over-estimation pattern indicates that the reading error increases as the measured resistance value increases. None of the combinations of R2 values produced relative errors below 2%, indicating that the device's accuracy starts to deviate from ideal performance in this range. The consistently positive error pattern also indicates that the error is not caused by noise fluctuations or external disturbances, but is most likely due to the effect of suboptimal linear calibration, similar to what occurred in the R1 = 20.1 Ω test.

The test on the 476.1 Ω reference resistor showed the same consistency of over-estimation as in the previous test, but with a much larger absolute error. Readings ranged from +7.81 to +16.87 Ω, with relative errors ranging from +1.64% to +3.54%, as shown in Table 7. Compared to the reference values, the accuracy of the device starts to decrease significantly, especially when R2 exceeds 1000 Ω. The relative error also continues to increase as R2 increases, indicating that the system's ability to compensate for the influence of R2 on the readings is no longer effective. Although the error value is still below 5%, the tool's performance in high-precision resistance measurement begins to show limitations in terms of accuracy. However, precision remains evident from the consistency of the over-estimation pattern.

The test at R1 = 1971.9 Ω showed that the accuracy improved slightly compared to the previous test. Although the absolute error reaches up to +36.88 Ω, the relative error remains below 2% across all R2 variations, as shown in Table 4 Since the resistance value is quite large, the high absolute error still results in a low relative error. However, the relative error pattern remains positive and increases as R2 increases, from +0.38% at R2 = 100 Ω to +1.87% at R2 = 2000 Ω. This indicates that the measurement system is still affected by changes in R2 configuration. The reading at R2 = 50 Ω shows a value lower than the reference (-0.09%), which is the only case of under-estimation in this line. Most likely, this is due to the non-optimal stabilization of the measurement when R_ground is very small. In general, the readings show a small relative error (< 2%) at high resistances, but the over-estimation pattern still appears as in the previous range. Although the relative error is not very large, the absolute value is quite significant for precision measurements, indicating that the tool design is capable of handling large resistances stably.

Based on the results of the ADS 1256 system test on six reference points with different R2 value variations:

- Range < 10Ω: Fluctuating, relatively high error, the influence of R2 is large.
- Range 10-100 *Omega*: Accuracy improves, but over-estimation starts to appear.
- Range > 0Ω: Systematic and increasing over-estimation, 2-4% relative error, influenced by configuration R2.

Reducing measurement error requires quantifying the maximum possible deviation in instrument output (Morris, 2001). In resistivity measurements, uncertainty estimation ensures data reliability and accuracy (White, 2008), and may arise from both random variations and system limitations (Stein et al., 2019). Based on a series of tests and analysis, the ADS1256-based resistance measurement system demonstrates good performance in the medium to high resistance (R1) range, but shows less accuracy at low resistance (R1). The reading discrepancy, especially at low resistances, is most likely due to the instability of the gain ratio of the voltage divider. Nevertheless, the maximum value of relative error (ε) at test resistance R1 = 1 Ω, which is 6.67%, is still within the permissible limit according to Table 2 as it is below 10.2%. The deviation of the readings also indicates the influence of the autorange mechanism, which is related to the gain setting. This mechanism automatically changes the internal measurement range when the current or voltage exceeds a certain threshold.

This phenomenon is illustrated in Figure 4 which pre-

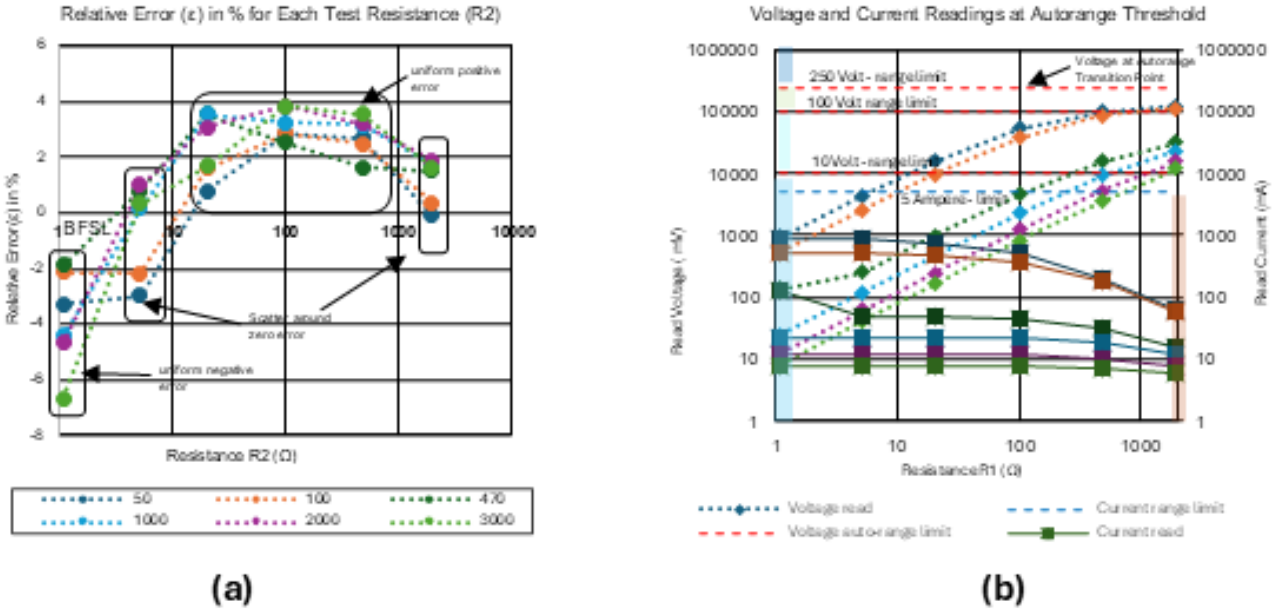

Figure 4. (a) Relative Error (ε) in % each R2 test resistance (b) voltage and current readings at autorange threshold

sents a uniform positive error observed in the measurement of resistance values within the range of R1 = 10 – 1000 Ω. Measurement of resistance in this range requires a relatively high voltage reading, while the corresponding current readings remain within the auto-range limits without exceeding the current measurement threshold. As shown in Figure 4(b), the voltage required to measure resistance values of 10 to 1000 Ω spans from approximately 100 mV to 100 V. Within this range, the voltage auto-range transition occurs between the 10 V and 100 V thresholds. The occurrence of this uniform positive error is presumed to be caused by a mismatch in the internal gain associated with the auto-range mechanism. The uniform positive error suggests that the discrepancy is not caused by random noise, but by internal bias in gain or scaling factors (Chen et al., 2024).

Figure 4(b) is seen by the voltage threshold data, which is more volatile than the current threshold. Such voltage fluctuations occur at range transition points and have the potential to affect the accuracy of resistance calculations, either in the form of underestimates or overestimates. Since the resistance calculation is highly dependent on the voltage-to-current ratio, improving the system's accuracy can be achieved by controlling the voltage reading range to minimize errors caused by the autorange mechanism. The subsequent performance evaluation reveals how this improvement impacts measurement accuracy and the instrument's potential for practical use

A comparative review of several previous studies was conducted, as presented in Figure 5, which illustrates the comparative analysis of relative error values (%) obtained from different ADC-based measurement systems. Figure 5(a) illustrates the comparison of the relative error (%) of voltage measurements on resistor R1 using the ADS1115 ADC against the reference instrument Bench UT61B. The measurements were carried out at two resistor values, namely 10 kΩ and 100 kΩ, represented by different symbols. For the 10 kΩ resistor, the relative error ranged from approximately -25% to near 0%, with an increasing trend as the measured voltage rose. Conversely, for the 100 kΩ resistor, the relative error was larger, starting at around -35% at low voltages and improving only to about -10% at higher voltages. This indicates that the ADS1115 provides better accuracy for medium resistance values around 10 kΩ compared to higher resistance values of 100 kΩ. The ADS1115 is therefore more suitable for measuring potential differences in low-resistance materials below 10 kΩ with a confidence level of 97%. However, for high-resistance materials above 10 kΩ, its performance is less reliable (Antosia, 2020).

Figure 5(b) illustrates the relationship between relative error (%) and voltage measurement points obtained using the 10-bit ADC on the Arduino UNO, compared with the reference instrument ZOYI ZT 102. At very low voltages (close to 0-200 mV), the relative error reached 35-40% due to the limited resolution of the ADC, which can only represent data with a precision of approximately 4.88 mV per step. As the voltage increased, the relative error decreased sharply and became more stable, particularly after exceeding 1000 mV. Within the medium-to-high voltage range (≥1 V), the relative error was below 2%, which can be considered sufficiently accurate for general applications. These results indicate that the Arduino UNO ADC is more suitable for medium-to-high voltage measurements, whereas very low voltage measurements require a higher-resolution ADC. Figure 5(c) shows the relative error (%) in resistance

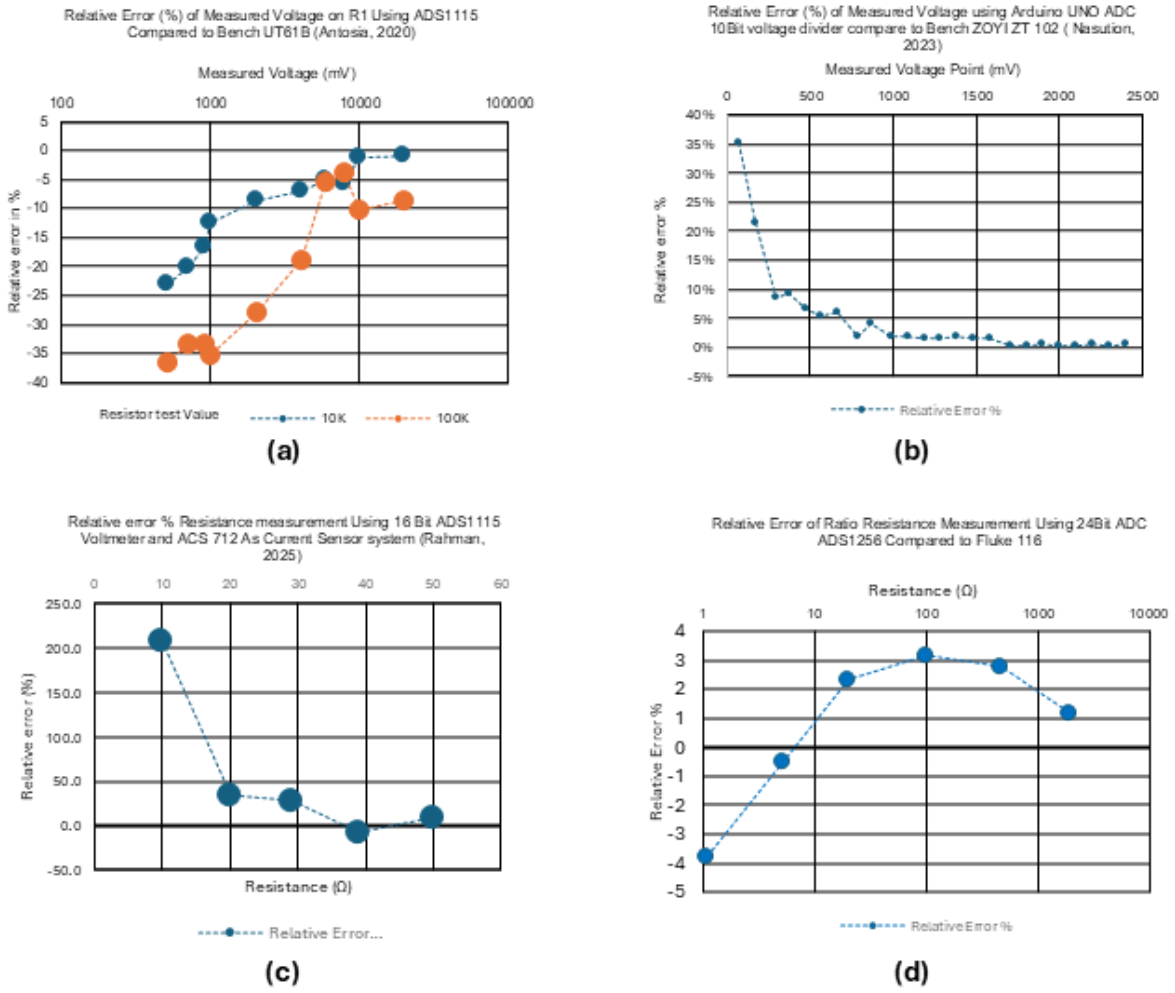

Figure 5. Comparison of relative error (%) across different ADC-based measurement systems: (a) variation of voltage measurements using the ADS1115 for medium-to-high resistance values of R1 (10 kΩ and 100 kΩ) compared to the bench multimeter UT61E (Antosia, 2020); (b) relative error (%) graph with voltage measurement points obtained using the 10-bit ADC on Arduino UNO (Nasution and Lubis, 2023); (c) resistance measurements using a hybrid configuration of the ADS1115 as a voltage sensor combined with the ACS712 current sensor (Rahman et al., 2025); and (d) relative error of R1 resistance readings in this study using the ADS1256, representing the average resistance values across all R2 ranges.

measurements using the ADS1115 16-bit voltmeter system combined with the ACS712 current sensor. At low resistance values (approximately 10 Ω), the relative error was very high, exceeding 200%, which highlights the system's limitations in accurately measuring small resistances. As the resistance increased to the range of 20-30 Ω, the relative error decreased drastically and approached 0%, indicating that the measurement results were closer to the true values. At 40 Ω, the relative error was slightly negative, around -20%, before returning closer to zero at higher resistance values. These results suggest that the system is more optimal for medium resistance measurements, while its accuracy deteriorates significantly for low resistance values.

Figure 5(d) presents the relative error (%) in resistance ratio measurements using the 24-bit ADS1256 ADC compared with the Fluke 116 multimeter. At low resistance values around 1 Ω, the relative error was negative (approximately -4%), indicating that the measurement result was lower than the reference value. As the resistance increased to about 100 Ω, the relative error rose positively to approximately +3%. Beyond this range, at higher resistances up to 1000 Ω the relative error decreased slightly but remained above zero, reflecting relatively good accuracy. Overall, this measurement system demonstrated more stable and accurate performance in the medium-to-high resistance range compared to the low resistance range. Comparison of Figure a-d. The comparative analysis of the four graphs demonstrates that ADC performance is strongly influenced by its resolution and the measurement application range. The 10-bit ADC on the Arduino UNO Figure 4(b) exhibited limitations at low voltages due to its 4.88 mV per-step resolution, resulting in high relative errors, although it remained sufficiently

accurate for medium-to-high voltages. The 16-bit ADS1115 Figure 4(a) and 4(c) provided better results for voltage measurements with a 10 kΩ resistor but showed significant errors for both high resistance and very low resistance when used with the ACS712 current sensor. In contrast, the 24-bit ADS1256 Figure 4d displayed the most stable performance, with small and consistent relative errors, particularly in the medium-to-high resistance range.

Based on the test results after implementing the optimized voltage range control, the developed geoelectrical instrument demonstrated a satisfactory level of accuracy. With this performance, the instrument has the potential to be utilized as a learning for instrumentation, both in theoretical courses and practical activities in the field of geophysical instrumentation. Furthermore, the measured error values remain within an acceptable range, enabling its application in field survey activities, provided that the instrument's internal error factors are taken into account during data interpretation.

4 CONCLUSION

Based on the test results using the ADS1256 system and test samples, the following conclusions were obtained:

(a) Voltage (mV) measurements show a wider range of variation and more fluctuating errors than
(b) The best accuracy is achieved over the range of resistance R1 (representing the resistance of the subsurface target) at medium to high resistances ($> 10\Omega$), while accuracy decreases dramatically at low resistances. The final error value of the resistance measurememt is in the range of 0.09% to a maximum of 6.67%.
(c) The condition of the resistance R2 (representing the surface resistance) affects the stability of the ADS1256 system reading, especially in the low resistance range.
(d) The nonlinearity of the readings is expected to come from an internal autorange mechanism in the voltage (mV) measurement, which requires further development and optimization.

ACKNOWLEDGEMENTS

The authors thank LPPM UPN "Veteran" Yogyakarta for research funding and the Department of Geophysical Engineering for providing laboratory facilities, equipment, and testing locations.

Pustaka

Antosia, R. (2020): Voltmeter design based on ads1115 and arduino uno for dc resistivity measurement. *JTERA (Jurnal Teknologi Rekayasa)*, **5**, 73, doi:10.31544/jtera.v5.i1.2019.73-80.

Azharudin, I., Imaddudin, I., Nuryadin, B. (2013): Rancang bangun alat geolistrik untuk menentukan jenis bahan di bawah permukaan bumi. *Jurnal Kajian Islam, Sains dan Teknologi*, **7**(1), e00122, ISSN 1979-8911.

Chen, Y., Huang, S., Huang, Q., Fan, Y. Yuan, J. (2024): The error analysis of bit weight self-calibration methods for high-resolution sar adcs. *IEEE Transactions on Very Large Scale Integration (VLSI) Systems*, **32**(11), 1983–1992, doi:10.1109/TVLSI.2024.3458071.

ChinalcTech (2023): Ads1256 24-bit 8 channel adc ad module high precision adc. doi:http://www.chinalctech.com/cpzx/Programmer/AD˙DA˙Module/546.html.

Clement, R., Fargier, Y., Dubois, V., Gance, J., Gros, E. Forquet, N. (2020): Ohmpi: An open source data logger for dedicated applications of electrical resistivity imaging at the small and laboratory scale. *HardwareX*, **8**, e00122, doi:10.1016/j.ohx.2020.e00122.

De-Carlo, L., Perkins, K. Caputo, M.C. (2021): Evidence of preferential flow activation in the vadose zone via geophysical monitoring. *Sensors*, **21**(4), ISSN 1424-8220, doi:10.3390/s21041358.

Fatima-Zohra, H., Laredj, N., Maliki, M., Missoum, H. Bendani, K. (2019): Laboratory evaluation of soil geotechnical properties via electrical conductivity evaluación de laboratorio de las propiedades geotécnicas del suelo mediante conductividad eléctrica. *Revista Facultad de Ingeniería*, **90**, 101–112, doi:10.17533/udea.redin.n90a11.

Hartono, H., Abdullatif, F., Nur Aziz, A., Sehah, S., Sugito, S. Silalahi, S. (2022): Rancang bangun data logger berbasis arduino sebagai penyimpan data. *Jurnal Teras Fisika*, **5**, 23, doi:10.20884/1.jtf.2022.5.2.6887.

Hazreek, Z.A.M., Azhar, A.T.S., Aziman, M., Fauzan, S.M.S.A., Ikhwan, J.M. Aishah, M.A.N. (2017): Forensic assessment on ground instability using electrical resistivity imaging (eri). *Journal of Physics: Conference Series*, **790**(1), 012038, doi:10.1088/1742-6596/790/1/012038.

Huda, F., Harmadi, H. Pohan, A. (2021): Prototipe rancang bangun alat geolistrik menggunakan arduino uno r3 dan transceiver nrf24l01+. *Jurnal Fisika Unand*, **10**, 435–444, doi:10.25077/jfu.10.4.435-442.2021.

Indarto, B., Sudenasahag, G.R., Rahmad, D.B., Basri, M.H. Sunarno, H. (2016): Rancang bangun sistem pengukuran resistivitas geolistrik dengan menggunakan sumber arus konstan. *Jurnal Fisika dan Aplikasinya*, **12**(2), 83–89, doi:http://dx.doi.org/10.12962"%2Fj24604682.v12i2.1125.

Kuklin, D. (2020): Device for the field measurements of frequency-dependent soil properties in the frequency range of lightning currents. *Review of Scientific Instruments*, **91**(11), 114701, ISSN 0034-6748, doi:10.1063/5.0012126.

Morris, A.S. (2001): 3 - errors during the measurement process. In: Morris, A.S. (Ed.) *Measurement and Instrumentation Principles (Third Edition)*. Butterworth-Heinemann, Oxford, third edition edn., ISBN 978-0-7506-5081-6, 32–63, doi:https://doi.org/10.1016/B978-075065081-6/50004-7.

Muhammad, A. Gunawan, H. (2016): Rancang bagun alat geolistrik berbasis pulse width modulation (pwm). *Prosiding Seminar Nasional Fisika (E-Journal)*, **5**, SNF2016–CIP, doi:10.21009/0305020127.

Nasution, M. Lubis, L.H.and Ramandan, T. (2023): Rancang bangun resistivity meter berbasis arduino uno dilengkapi dengan data logger sebagai penyimpan data. *Navigation Physics: Jurnalof Physics Education)*, **5**(2).

Rahman, A., Nurfalaq, A. Manrulu, R.H. (2025): Rancang bangun alat ukur resistivitymeter berbasis arduino. *Applied Phsyics of Cokroaminoto Palopo Journal*, **6**(1).

Saad, R., Nawawi, M.N.M., Muztaza, N.M. Jusoh, Z. (2010): Testing of resistivity imaging method with different protocols to detect void using miniature model. *AIP Conference Proceedings*, **1250**(1), 177–180, ISSN 0094-243X, doi:10.1063/1.3469629.

Setiawan, D., Prayatman, R. S., T. (2024): Design of resistivity meter data storage system based on arduino mega 2560 laboratory scale measurement results. *Indonesia Journal of Applied Physics*, **14**(1).

Stein, M., Haselberg, R., Mozafari-Torshizi, M. Wätzig, H. (2019): Experimental design and measurement uncertainty in ligand binding studies by affinity capillary electrophoresis. *ELECTROPHORESIS*, **40**(7), 1041–1054, doi:https://doi.org/10.1002/elps.201800450.

Telford, W.M., Geldart, L.P. Sheriff, R.E. (1990): Applied Geophysics. Cambridge University Press, 2nd edn.

White, G.H. (2008): Basics of estimating measurement uncertainty. *The Clinical biochemist. Reviews*, **29 Suppl 1**, S53–60, doi:https://pubmed.ncbi.nlm.nih.gov/18852859/.

Zhao, R. Anderson, N. (2018): A description of field setup and common issues in 2-d electrical resistivity tomography data acquisition. *International Journal of Science and Research (IJSR)*, **7**, 1061–1066, doi:10.21275/ART20193810.